THE ASTROPHYSICAL JOURNAL, 278:L19–L22, 1984 March 1

INFRARED CIRRUS: NEW COMPONENTS OF THE EXTENDED INFRARED EMISSION[1]

F. J. LOW, D. A. BEINTEMA, T. N. GAUTIER, F. C. GILLETT, C. A. BEICHMAN, G. NEUGEBAUER, E. YOUNG, H. H. AUMANN, N. BOGGESS, J. P. EMERSON, H. J. HABING, M. G. HAUSER, J. R. HOUCK, M. ROWAN-ROBINSON, B. T. SOIFER, R. G. WALKER, AND P. R. WESSELIUS

Received 1983 September 12; accepted 1983 November 21

ABSTRACT

Extended sources of far-infrared emission superposed on the zodiacal and galactic backgrounds are found at high galactic latitudes and near the ecliptic plane. Clouds of interstellar dust at color temperatures as high as 35 K account for much of this complex structure, but the relationship to H I column density is not simple. Other features of the extended emission show the existence of warm structures within the solar system. Three bands of dust clouds at temperatures of 150–200 K appear within 10° on both sides of the ecliptic plane. Their ecliptic latitudes and derived distances suggest that they are associated with the main asteroid belt. A third component of the 100 μm cirrus, poorly correlated with H I, may represent cold material in the outer solar system or a new component of the interstellar medium.

Subject headings: infrared: general — interplanetary medium — interstellar: matter

I. INTRODUCTION

In addition to discrete sources, the infrared sky, as seen by *IRAS*, is characterized by extended thermal emission from dust within the solar system and from within the Galaxy. The zodiacal emission and the smooth high galactic latitude emission from the Galaxy are described by Hauser *et al.* (1984); here we are concerned with a complex of extended sources superposed on this continuous background. These highly structured extended sources, which may be described as "infrared cirrus," are seen predominantly, but not exclusively, at 60 and 100 μm and may originate either in the interplanetary medium, the outer solar system, or the interstellar medium. Based on the relatively small amount of *IRAS* data available at this time, we have identified at least three classes of phenomena: (1) thermal emission at 60 or 100 μm, or both, that is positionally associated with the strongest concentrations of gas and dust at very high galactic latitudes as indicated by H I studies (Burstein and Heiles 1982); (2) large, relatively warm features associated with the ecliptic; (3) cold clouds, which are poorly correlated with known interstellar gas clouds and therefore may be new parts of the outer solar system or new structures within the interstellar medium.

As the result of model calculations (see, for example, Spencer and Leung 1978; Mezger, Mathis, and Panagia 1982), it is expected that in optically thin interstellar clouds the range of physical temperatures for graphite grains that are heated only by the interstellar radiation field (ISRF) should be 25–35 K; since the absorption efficiency, Q_{IR}, is proportional to ν^2, color temperatures, T_c, as high as 50 K may be expected. On the other hand, silicate grains, with Q_{IR} proportional to ν, are expected to be much colder, $T_c = 16$ K. Thus *IRAS*, with its capacity to measure both far-infrared surface brightness and temperature in the critical range for such clouds, promises to give optical depths and basic grain discrimination for a large variety of interstellar conditions.

[1] The *Infrared Astronomical Satellite* (*IRAS*) used in these observations was developed and is operated by the Netherlands Agency for Aerospace Programs (NIVR), the US National Aeronautics and Space Administration (NASA), and the UK Science and Engineering Research Council (SERC).

II. EMISSION FROM INTERSTELLAR DUST AT HIGH GALACTIC LATITUDES

Figure 1 shows an analog representation of six 100 μm detector outputs for one of the four regions of very high galactic latitude emission (region D in Table 1) that we discuss. Note that this region of sky was scanned twice, in two consecutive survey orbits, with different sets of detectors, resulting in quadruple coverage. This allows us to examine in detail the outputs of spatially overlapping detectors as they scan a complex region of weak diffuse emission. The sensitivity and repeatability of *IRAS* for very low frequency signals of this type is clearly evident in this small, but representative, selection of data.

Table 1 summarizes our observations of four high galactic latitude regions where the H I emission is at or near local maxima. The absolute calibration and reduction procedures are discussed by Neugebauer *et al.* (1984); uncertainties in the flux densities given here are less than 30%. Region A was selected because it has the highest concentration of atomic hydrogen in the polar regions mapped by Heiles (1975); B and D are essentially the next highest. In contrast, region C was found by visual inspection of the 100 μm data. Regions C and B are both included in the scan of Figure 2*b*. For comparison, we also include the H I column density expressed in BH units (Burstein and Heiles 1982). From the model calculations of Spencer and Leung (1978), we find that the ratio of flux densities at 60 and 100 μm should be approximately 0.55 for graphite grains and approximately 0.03 for silicate grains. The observed flux density ratio in the four clouds ranges from 0.18

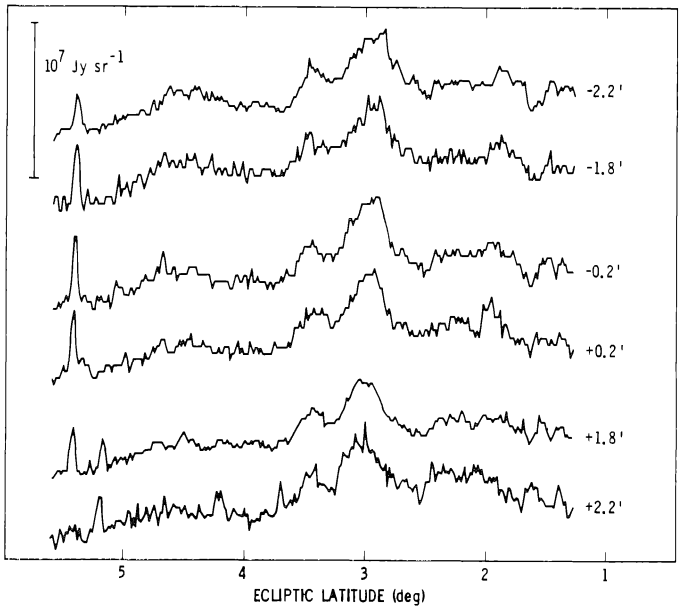

FIG. 1.—Outputs from six different 100 μm detectors crossing region D (see text). Alternate traces are from two consecutive orbits. The traces are labeled with their offsets in ecliptic longitude with respect to longitude 168°.32.

to 0.35; if the intensity of the ISRF is uniform, each cloud must contain a mixture of the two types of grains. In Table 2, relevant calculated quantities are given, including the emission optical depth at 100 μm, τ_{100}, and the values of A_v from Burstein and Heiles (1982). The ratio A_v/τ_{100} is remarkably constant for these clouds, with values lying in the commonly accepted range (Hildebrand 1983). In order to deduce a physical temperature, T_p, for the average grain, we have used $\nu^{1.5}$ for the emissivity dependence. The integrated infrared surface brightness was compared to the Werner and Salpeter (1969) value for the ISRF and was found to be consistent with the albedo of the cloud deduced from the value of A_v.

The results from these four clouds are in good agreement with theoretical expectations and help determine important grain and cloud properties. It is necessary, however, to emphasize that the relationship between H I column densities and infrared cirrus is not always as straightforward as indicated by this small subset of the data. As discussed below, there are regions of relatively prominent 100 μm emission with only weak H I, and there are many structures in the H I maps that do not appear prominently in the 100 μm scans.

III. WARM STRUCTURES IN THE INTERPLANETARY MEDIUM

An unexpected feature of the interplanetary medium has been found in all four wavelength bands. Figure 2 illustrates the effects that are seen as a half-degree beam, synthesized by averaging all detectors in a given band, is scanned across the ecliptic plane at four different longitudes. For a large-scale illustration of the character of these pole-to-pole scans, see the *Letter* by Hauser *et al.* (1984). The flat-top or "mesa" structure accompanied by shoulders on each side of the plane is the normal characteristic of these scans. This is clearly seen in the scans shown in Figures 2*a*, 2*b*, and 2*c*, which are widely separated in ecliptic longitude. Figure 2*d* shows an example of the observed variation in the characteristic mesa and shoulder pattern. These features appear at 12, 25, and 60 μm as three parallel bands of emission when the underlying smooth component of zodiacal emission has been subtracted from each scan.

These three warm bands of zodiacal dust run nearly continuously around the solar system with some degree of interruption or change in strength and temperature. The ratio of these features to the underlying smooth component of the zodiacal emission is not the same at all longitudes. It is quite likely that appreciable changes due to orbital and parallactic effects will be seen on *IRAS* rescans taken approximately 6 months after the scans presented here.

After subtracting the smooth component of the zodiacal emission from the scans at 12, 25, and 60 μm, an estimate of the typical surface brightness for each of the three bands yields the set of color temperatures, T_c, listed in Table 3; the mean optical depth is approximately 10^{-8}. For comparison, the last column in Table 3 gives the distances from the Sun for large, rapidly rotating, gray particles in radiative equilibrium at the observed temperatures. It appears that the material responsible for these zodiacal dust bands is associated with the main asteroid belt. This agrees well with the notion that small grains within the solar system are formed in collisions between asteroids in the main belt. However, at present we can only speculate concerning the origin of the two outer bands of dust which are symmetrically located on each side of the central band.

IV. COLD UNIDENTIFIED CIRRUS

Although much of the structure near the ecliptic seen in the 100 μm scans shown in Figure 2 appears to be connected with the warm bands discussed above, we also find degree-size

TABLE 1

OBSERVATIONS OF HIGH GALACTIC LATITUDE CLOUDS

Cloud	Galactic Coordinates		H I (BH)	Peak Brightness (MJy sr^{-1})		T_c (60/100) (K)	Approx. Size
	l	b		60 μm	100 μm		
A	129°.7	−69°.4	275	3.0	10	34	2°.5
B	273.0	74.7	225	0.79	4.3	28	2.8
C	272.7	81.7	175	0.20	1.3	26	0.3
D	252.9	61.4	225	1.0	4.9	29	1.0

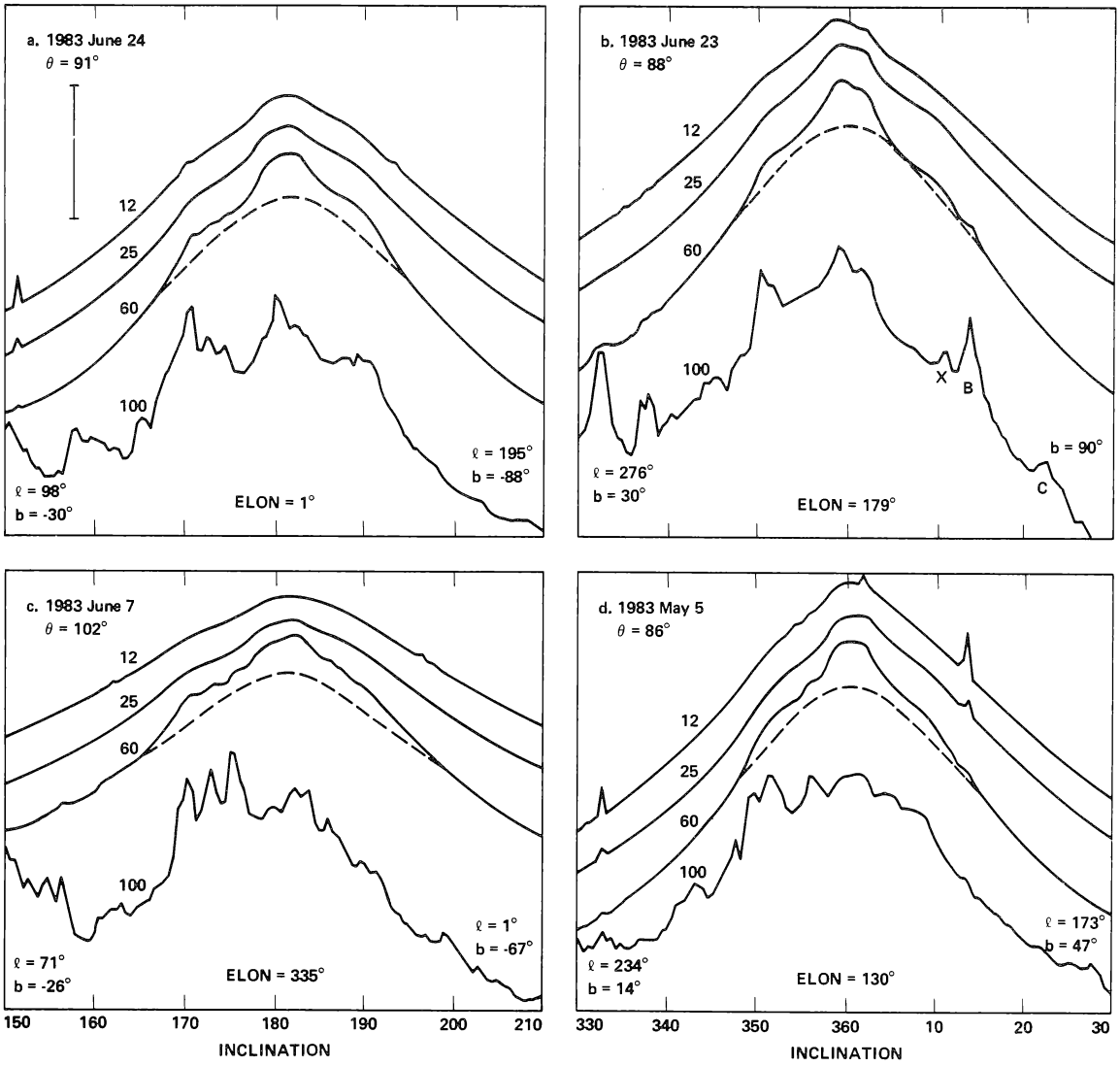

FIG. 2.—Half-degree beam scans crossing the ecliptic at four different longitudes (ELON), showing "mesa" and "shoulder" structures in the four wavelength bands. The scans have been suppressed by arbitrary amounts. Dashed curves representing the smooth component of the zodiacal emission at 60 μm are included for illustration only; detailed modeling has not been performed. The parameter θ is the constant angle from the Sun vector; inclination measures the rotation about that vector. The ecliptic is at inclinations 0° and 180°. The ends of the depicted portions of the scans are marked with their galactic coordinates. The vertical bar in (*a*) corresponds to 12, 30, 10, and 6 MJy sr^{-1} in the four bands, assuming spectra are flat in F_ν. The letters labeling 100 μm features in (*b*) refer to regions discussed in the text.

TABLE 2

CALCULATED PROPERTIES OF HIGH GALACTIC LATITUDE CLOUDS

Cloud	T_p (K)	τ_{100} (10^{-5})	A_v (mag)	A_v/τ (mag)
A	27	5	0.18	3500
B	23	6	0.13	2300
C	21	3	0.07	2300
D	23	6	0.13	2000

TABLE 3

WARM BANDS IN THE INTERPLANETARY MEDIUM

BAND	ECLIPTIC COORDINATES		T_c (K)	D (AU)
	Lat.	Long.		
South	−10°6	1°3	200	2.2
Central ...	−2.8	1.3	195	2.3
North	9.0	1.3	165	3.2

regions of emission only at 100 μm that are not correlated with these features of the solar system or with known structures in the Galaxy. The cold source labeled X in Figure 2*b* is not associated with the warm interplanetary material and has no corresponding peak in the Heiles (1975) map. Indeed, much of the structure seen so prominently in the 100 μm scans is in this category. This dust emission could, perhaps, be associated with H I at anomalous velocities, with small amounts of molecular rather than atomic hydrogen, or with cold material in the outer solar system. Fortunately, the *IRAS* mission plan of rescanning the sky after an interval of 6 months is well suited to distinguish between dust clouds in orbit around the Sun at various distances and distant interstellar clouds. This aspect of the infrared cirrus remains one of the most enigmatic characteristics of the sky as seen by *IRAS* and will continue as such until the sky has been examined a second time.

Many people deserve great credit for their contributions to *IRAS*; however, it is fitting that we acknowledge here those individuals who had the courage and skills to rebuild the focal plane so that it could produce the data used in studies of the kind presented in this *Letter*. T. N. G. was supported by an NRC Resident Research Associateship for this work.

REFERENCES

Burstein, D., and Heiles, C. 1982, *A.J.* **87**, 1165.
Hauser, M. G., *et al.* 1984, *Ap. J.*, **278**, L15.
Heiles, C. 1975, *Astr. Ap. Suppl.*, **20**, 37.
Hildebrand, R. H. 1983, *Quart. J. R.A.S.*, **24**, 267.
Mezger, P., Mathis, J., and Panagia, N. 1982 *Astr. Ap.*, **105**, 372.
Neugebauer, G., *et al.* 1984, *Ap. J.* (*Letters*), **278**, L1.
Spencer, R. G., and Leung, C. M. 1978, *Ap. J.*, **222**, 140.
Werner, M. W., and Salpeter, E. E. 1969, *M.N.R.A.S.*, **145**, 249.